Renormalized polarizability in the Maxwell Garnett theory

Rubén G. Barrera*
Departamento de Física, Centro de Investigación y Estudios Avanzados del Instituto Politécnico Nacional, 07000 México, Distrito Federal, Mexico

Guillermo Monsivais and W. Luis Mochán
Instituto de Física, Universidad Nacional Autónoma de México, Apartado Postal 20-364, 01000 México, Distrito Federal, México
(Received 10 July 1987; revised manuscript received 11 February 1988)

We develop a simple theory for the macroscopic dielectric function of a system of identical spheres embedded in a homogeneous matrix within the dipolar long-wavelength approximation. We obtained a relationship similar to the Clausius-Mossotti relation, but with a renormalized polarizability for the spheres instead of the bare polarizability. This renormalized polarizability obeys a second-order algebraic equation and it is given in terms of the bare polarizability, the volume fraction, and a functional of the two-particle correlation function of the spheres. We calculate the optical properties of metallic spheres within an insulating matrix and we compare our results with previous theories and with experiment.

I. INTRODUCTION

The study of the optical properties of composite materials made of small metallic particles embedded in an insulating matrix continues to attract the attention of many investigators both theoretically[1–19] and experimentally.[20–29] Although the problem is very old[30] and significant advances have been achieved a definite solution has still not been found. It has been recognized[31] that part of its complexity is the strong dependence of the optical properties of the system on the geometry and topology of its microstructure. Even for the apparently simple geometry of isolated and evenly distributed identical spherical particles of radius much smaller than the wavelength of light, the solution of the problem is far from being settled. In this case the theoretical problem is that of finding the effective dielectric response of the system in terms of the dielectric functions of the metallic sphere and the insulating matrix and the statistical properties of the distribution of particles which are determined by the sample preparation process. This is the problem that will be analyzed in this paper.

One of the first and most fruitful solutions to this problem was obtained by Maxwell Garnett[30] and it is known nowadays as the Maxwell Garnett theory (MGT). In this theory the fluctuations of the local field are completely neglected. Most of the work done thereafter has attempted to take into account the effects of these fluctuations. A number of theories have been formulated in the language of multiple-scattering theory. It has been shown[32] that MGT corresponds to the quasistatic dipolar limit of either the average-t-matrix approximation (ATA) used in the electronic theory of alloys[33] or the quasicrystalline approximation (QCA) used in the scattering theory of disordered systems.[34] These approximation have been extended to include retardation and higher multipoles,[35] the nonlocal response of the metal,[7] and by proposing more elaborate approximation schemes.[1,2,4,5,8–10,14,15,17,18] Other approaches to the problem include cluster expansions,[3,6,11] spectral representations,[18] or the replacement of spatial disorder by substitutional disorder.[9]

The main results obtained so far in the long-wavelength limit for isolated metallic spheres embedded in a dispersionless insulating matrix are that the surface-plasmon resonance in the imaginary part of the effective dielectric response as a function of frequency becomes redshifted and asymmetrically broadened with respect to the one predicted by MGT.[1,4,9] While in MGT the position of the resonance depends only on the volume fraction of the spheres and its width on the relaxation time of the Drude contribution to the dielectric function, more elaborate theories[1,4] show that they also depend on the two-particle distribution function of the spheres. This is due to their multiple-scattering character and their dependence on the local-field fluctuations.

An accurate comparison between theory and experiment is still open to question due to the fact that the models used until now do not incorporate all the features of the actual experimental systems. Nevertheless, experimental measurements[25,27] on systems of noble-metal small particles in insulating matrices show a redshift and an asymmetric broadening of the surface-plasmon resonance in reasonable agreement with recent theoretical results.[1,4,9]

In Sec. II of this paper we develop a theory, within the quasistatic dipolar approximation, for the effective dielectric function of a system of identical spheres of radius a_0 with polarizability α embedded in a medium with dielectric function ϵ_b. We show that by using a simple approximation for the contribution of the local-field fluctuations we obtain a relation of the Clausius-Mossotti type, but with a renormalized polarizability α^* instead of α. This renormalized polarizability obeys an algebraic quadratic

equation with coefficients which depend on the polarizability α, the volume fraction of the spheres, and a functional of the two-particle distribution function of the system. Our theory could also be useful in a closely related problem: that of the calculation of the macroscopic (effective) dielectric function of liquids and dense gases in thermal equilibrium.[36] In that case α would be the molecular polarizability which could be obtained quantum mechanically and the distribution functions could be calculated using statistical mechanics. As additional complications one would have the correlations due to the quantum nature of the molecular polarizability. This problem is also very old[37] and a vast amount of different calculation procedures have been devised which involve polarizability or density expansions,[38] cluster expansions,[39,40] integral equations,[41] and their extensions to include the dependence of the molecular polarizability on density,[42] etc.

In Sec. III we apply our theory to spheres with a Drude-type dielectric function embedded in gelatin. We analyze the dependence of the position and the line shape of the surface-plasmon resonance on the two-particle distribution function by comparing results for the hole correction (HC), Percus-Yevick (PY), and molten copper (MCu) two-site distribution functions. We also compare our results with those derived from other theories and with experiment. Finally, Sec. IV is devoted to conclusions.

The main merit of our theory is its simplicity and a clear physical picture of the main approximation. Our results are similar to ones obtained with more complicated calculations[1,4,9] and they are in reasonable agreement with experiment.[25]

II. THEORY

We consider an ensemble of $N \gg 1$ identical spheres of radius a_0 with polarizability $\alpha = a_0^3(\epsilon_s - \epsilon_b)/(\epsilon_s + 2\epsilon_b)$, which is the polarizability of an isolated sphere with dielectric function ϵ_s within a medium with dielectric function ϵ_b. The centers of the spheres are located at positions $R_1, R_2, \ldots, R_N$ and the system is in the presence of an external electric field $E^{\rm ex}$ oscillating with frequency ω. We assume $a_0 \ll \omega/c$, where c is the speed of light, so that the dipole moment $\mathbf{p}_i$ induced on the ith sphere obeys

$$\mathbf{p}_i(\omega) = \alpha(\omega)\left[\mathbf{E}_i^0 + \sum_j \overleftrightarrow{t}_{ij}\cdot\mathbf{p}_j(\omega)\right] , \tag{1a}$$

where $\mathbf{E}_i^0$ is the electric field induced within the medium at $\mathbf{R}_i$ in the absence of the spheres and

$$\overleftrightarrow{t}_{ij} = (1-\delta_{ij})\nabla_i\nabla_j(1/R_{ij}) \tag{1b}$$

is the dipole-dipole interaction tensor in the quasistatic limit. Here $R_{ij} \equiv |\mathbf{R}_i - \mathbf{R}_j|$ and δ_{ij} is the Kronecker δ function.

The effective or macroscopic dielectric response $\overleftrightarrow{\epsilon}_M$ of the system is defined by

$$\langle \mathbf{D}\rangle(\mathbf{r},t) = \int\int \overleftrightarrow{\epsilon}_M(\mathbf{r},\mathbf{r}';t-t')\cdot\langle \mathbf{E}\rangle(\mathbf{r}',t')d^3r'dt' , \tag{2}$$

where $\mathbf{D}$ and $\mathbf{E}$ are the displacement and electric field, respectively, and $\langle\ \rangle$ means average. Here we will use an ensemble average over the collection of positions $\{\mathbf{R}_i\}$ of the spheres. We assume that the ensemble is homogeneous, isotropic, and invariant under inversions. Then $\overleftrightarrow{\epsilon}_M$ is a function of $|\mathbf{r}-\mathbf{r}'|$ and its Fourier transform in space and time $\overleftrightarrow{\epsilon}_M(q,\omega)$ can be written as[43]

$$\overleftrightarrow{\epsilon}_M(q,\omega) = \epsilon_M^l(q,\omega)\hat{\mathbf{q}}\hat{\mathbf{q}} + \epsilon_M^t(q,\omega)(1-\hat{\mathbf{q}}\hat{\mathbf{q}}) , \tag{3}$$

where $\mathbf{q}$ is the wave vector and $\hat{\mathbf{q}} = \mathbf{q}/q$. Here and in the following the superscripts l and t denote longitudinal and transverse projections, respectively. For example, $\epsilon_M^l \equiv \hat{\mathbf{q}}\cdot\overleftrightarrow{\epsilon}_M\cdot\hat{\mathbf{q}}$ and $E^l \equiv \hat{\mathbf{q}}\cdot\mathbf{E}$. Our purpose is the calculation of the *local* macroscopic dielectric response $\epsilon_M(\omega)$ defined by[44]

$$\epsilon_M(\omega) = \lim_{q\to 0}\epsilon_M^l(q,\omega) = \lim_{q\to 0}\epsilon_M^t(q,\omega) . \tag{4}$$

Since in our case the collection of polarizable spheres is embedded in a medium with local dielectric function $\epsilon_b(\omega)$, it can be shown that

$$\langle D\rangle^l(q,\omega) = \epsilon_b(\omega)[\langle E\rangle^l(q,\omega) + 4\pi n\langle P\rangle^l(q,\omega)] , \tag{5a}$$

where $n\langle \mathbf{P}\rangle(q,\omega)$ is the Fourier transform of the average polarization field

$$n\langle \mathbf{p}\rangle(r;\omega) = \left\langle \sum_i \mathbf{p}_i(\omega)\delta(\mathbf{r}-\mathbf{R}_i)\right\rangle , \tag{5b}$$

and n is the number density of spheres. Now using Eq. (5), the symmetry properties of the ensemble, and taking into account that $\langle D\rangle^l$ is equal to the longitudinal protection $E^{{\rm ex},l}$ of the external field, we obtain

$$\frac{\epsilon_b(\omega)}{\epsilon_M(\omega)} = 1 - 4\pi\epsilon_b(\omega)[\lim_{q\to 0}\chi^{{\rm ex},l}(q,\omega)] , \tag{6a}$$

where $\chi^{\rm ex}(q,\omega)$ is the external susceptibility defined by

$$n\langle \mathbf{P}\rangle(q,\omega) = \chi^{\rm ex}(q,\omega)\mathbf{E}^{\rm ex}(q,\omega) . \tag{6b}$$

Thus the relationship between $\epsilon_M(\omega)$ and the microscopic parameters of our system can be obtained by calculating $\chi^{{\rm ex},l}(q\to 0,\omega)$.

The main advantage of Eq. (6), in comparison with other approaches,[11,40,45] is that it provides a well-defined procedure for the calculation of $\epsilon_M(\omega)$ directly in terms of a response to the *external* field. This removes the need of identifying the macroscopic electric field $\langle \mathbf{E}\rangle$ during the calculation. Also, the introduction of the supplementary length $1/q$ eliminates the appearance of shape-dependent or conditionally convergent integrals.[32]

Since there is no macroscopic l-t coupling due to the symmetry properties of the ensemble, the calculation of $\chi^{{\rm ex},l}(q,\omega)$ can be most easily done by exciting the microscopic system with an external longitudinal electric field with a single Fourier component,

$$\mathbf{E}^{\rm ex}(\mathbf{r}) = \hat{\mathbf{q}}E^{\rm ex}e^{i\mathbf{q}\cdot\mathbf{r}} . \tag{7}$$

In this case

$$\langle \mathbf{P}_i(\mathbf{q})\rangle \equiv \langle \mathbf{p}_i e^{-i\mathbf{q}\cdot\mathbf{R}_i}\rangle = \langle \mathbf{P}\rangle(q) \tag{8a}$$

is independent of i due to the translational invariance of the ensemble and $\mathbf{P}_i(\mathbf{q})\equiv\mathbf{p}_i e^{-i\mathbf{q}\cdot\mathbf{R}_i}$ satisfies

$$\mathbf{P}_i(\mathbf{q})=\alpha\left[\hat{\mathbf{q}}E^{\mathrm{ex}}/\epsilon_b+\sum_j \overleftrightarrow{\mathrm{T}}_{ij}(\mathbf{q})\cdot\mathbf{P}_j(\mathbf{q})\right], \tag{8b}$$

where

$$\overleftrightarrow{\mathrm{T}}_{ij}(\mathbf{q})=e^{-i\mathbf{q}\cdot(\mathbf{R}_i-\mathbf{R}_j)}\overleftrightarrow{t}_{ij} \tag{8c}$$

and we have omitted the argument ω. In that follows we will also omit the argument q unless it leads to confusion.

We now rewrite Eq. (8) as

$$\mathbf{P}_i=\alpha\left[\hat{\mathbf{q}}E^{\mathrm{ex}}/\epsilon_b+\sum_j \overleftrightarrow{\mathrm{T}}_{ij}\cdot\langle\mathbf{P}\rangle+\sum_j \overleftrightarrow{\mathrm{T}}_{ij}\cdot(\mathbf{P}_j-\langle\mathbf{P}\rangle)\right] \tag{9a}$$

$$\equiv\alpha\left[\mathbf{E}'_i+\sum_j \overleftrightarrow{\mathrm{T}}_{ij}\cdot\Delta\mathbf{P}_j\right], \tag{9b}$$

where $\Delta\mathbf{P}_j\equiv\mathbf{P}_j-\langle\mathbf{P}\rangle$ is the fluctuation of the jth dipolar moment. Here we have written the local field at $\mathbf{R}_i$ as the superposition of two fields: the fluctuating field $\mathbf{E}'_i$ generated by a system made up of average dipoles located at random positions $\{\mathbf{R}_j\}$ plus the field generated by the dipolar fluctuations $\Delta\mathbf{P}_j$ located at these same positions.

We define the renormalized polarizability tensor $\overleftrightarrow{\alpha}^*_i$ through the equation

$$\mathbf{P}_i=\overleftrightarrow{\alpha}^*_i\cdot\mathbf{E}'_i\ , \tag{10}$$

where the effects produced by the dipolar fluctuations in the local field are now contained within $\overleftrightarrow{\alpha}^*_i$, which depends on i and on the member of the ensemble and is therefore a fluctuating quantity. Its complete determination requires the dipolar moments $\{\mathbf{P}_j\}$ for each member of the ensemble for three linearly independent directions of the external field. Thus the reformulation of the problem in terms of the renormalized polarizability will not be useful unless we are able to propose a suitable approximation scheme. Here we investigate the consequences of the following approximation:

$$\overleftrightarrow{\alpha}^*_i\simeq\alpha^*\overleftrightarrow{\mathbb{1}}\ , \tag{11}$$

where $\mathbb{1}$ is the unit tensor and α^* is independent of i and is constant throughout the ensemble. This amounts to consider, according to Eq. (10), that the dipole moments $\mathbf{P}_i$ are directly proportional to the fluctuating field $\mathbf{E}'_i$.

It can be seen that setting $\alpha^*=\alpha$ corresponds to a complete disregard of the field generated by the dipolar fluctuations $\Delta\mathbf{P}_j$. This would only be appropriate for a perfect crystal since the dipolar fluctuations arise from spatial disorder. Our aim is then to determine the renormalized polarizability α^* including, in the best possible way, the contribution of these fluctuations. But before that we will derive the relationship between α^* and the macroscopic dielectric function ϵ_M.

First we substitute Eq. (11) into Eq. (10), then we take an ensemble average and the longitudinal projection of the resulting equation in order to obtain

$$\langle P\rangle^l=\alpha^*\left[E^{\mathrm{ex}}/\epsilon_b+\left\langle\sum_j T^l_{ij}\right\rangle\langle P\rangle^l\right], \tag{12}$$

where we have used the definition of $\mathbf{E}'_i$ given by Eq. (9), the translation invariance of the ensemble, and the fact that the ensemble average and the longitudinal projection commute.[44] Then we solve for $\langle P\rangle^l$ and we get

$$\langle P\rangle^l=\frac{\alpha^*}{1-\alpha^*\left\langle\sum_j T^l_{ij}\right\rangle}(E^{\mathrm{ex}}/\epsilon_b)\ . \tag{13}$$

Since[46]

$$\lim_{q\to0}\left\langle\sum_j T^l_{ij}(q)\right\rangle=-\frac{8\pi}{3}n\ , \tag{14}$$

then Eqs. (6) and (13) yield a relationship between α^* and ϵ_M of the Clausius-Mossotti (CM) type,[47]

$$\frac{\epsilon_M-\epsilon_b}{\epsilon_M+2\epsilon_b}=f\tilde{\alpha}^*\ , \tag{15}$$

but with the unitless renormalized polarizability $\tilde{\alpha}^*\equiv\alpha^*/a_0^3$ instead of $\tilde{\alpha}\equiv\alpha/a_0^3$. Here $f\equiv n(4\pi a_0^3/3)$ is the volume fraction of the spheres. We remark that several approximations to the macroscopic response can be written in a similar way but with different interpretations for the renormalized polarizability.[38]

Obviously the choice $\alpha^*=\alpha$ will bring us back to the usual CM relation or to the equivalent Maxwell-Garnett theory when $\tilde{\alpha}$ is substituted by $(\epsilon_s-\epsilon_b)/(\epsilon_s+2\epsilon_b)$. This means that MGT neglects completely the contribution of the field generated by the dipolar fluctuations.

Now we proceed to calculate α^*. In other aproaches a series expansion for α^* in terms of α or n is generated by successive iterations of Eq. (9). Here, instead, we close this system of equations by demanding self-consistency between Eqs. (10) and (11) with (8b), which becomes

$$\mathbf{P}_i=\alpha\left[\hat{\mathbf{q}}E^{\mathrm{ex}}/\epsilon_b+\alpha^*\sum_j \overleftrightarrow{\mathrm{T}}_{ij}\cdot\left[\hat{\mathbf{q}}E^{\mathrm{ex}}/\epsilon_b+\sum_k \overleftrightarrow{\mathrm{T}}_{jk}\cdot\langle\mathbf{P}\rangle\right]\right], \tag{16}$$

where the definition of E'_i given by Eq. (9) has been used. An ensemble average and the longitudinal projection of this equation yields

$$\langle P\rangle^l=\alpha\left[\left[1+\alpha^*\left\langle\sum_j T^l_{ij}\right\rangle\right](E^{\mathrm{ex}}/\epsilon_b)+\alpha^*\left\langle\sum_{j,k}\hat{\mathbf{q}}\cdot\overleftrightarrow{\mathrm{T}}_{ij}\cdot\overleftrightarrow{\mathrm{T}}_{jk}\cdot\hat{\mathbf{q}}\right\rangle\langle P\rangle^l\right]. \tag{17}$$

Finally, we substitute Eq. (13) in both sides of Eq. (17) and then take the $q\to0$ limit, obtaining the second-order algebraic equation

$$\frac{\alpha^*}{\alpha}=1+(\alpha^*)^2\lim_{q\to0}\Delta T^2(q)\ , \tag{18a}$$

which gives α^* in terms of α and the longitudinal projection of the fluctuation of the dipolar interaction

$$\Delta T^2(q)\equiv\left\langle\sum_{j,k}\hat{\mathbf{q}}\cdot\overleftrightarrow{\mathrm{T}}_{ij}(q)\cdot\overleftrightarrow{\mathrm{T}}_{jk}(q)\cdot\hat{\mathbf{q}}\right\rangle-\left\langle\sum_j\hat{\mathbf{q}}\cdot\overleftrightarrow{\mathrm{T}}_{ij}(q)\cdot\hat{\mathbf{q}}\right\rangle^2. \tag{18b}$$

The calculation of the dipolar fluctuation can be per-

formed in terms of distribution functions.

The first term in the right-hand side (rhs) of Eq. (18b) is given by

$$\left\langle \sum_{j,k} \hat{\mathbf{q}}\cdot\overleftrightarrow{\mathbf{T}}_{ij}\cdot\overleftrightarrow{\mathbf{T}}_{jk}\cdot\hat{\mathbf{q}} \right\rangle = n^2 \int\int \hat{\mathbf{q}}\cdot\overleftrightarrow{\mathbf{T}}_{12}\cdot\overleftrightarrow{\mathbf{T}}_{23}\cdot\hat{\mathbf{q}}\,\rho^{(3)}(\mathbf{R}_1,\mathbf{R}_2,\mathbf{R}_3)d^3R_2 d^3R_3 + n\int \hat{\mathbf{q}}\cdot\overleftrightarrow{\mathbf{T}}_{12}\cdot\overleftrightarrow{\mathbf{T}}_{21}\cdot\hat{\mathbf{q}}\,\rho^{(2)}(\mathbf{R}_1,\mathbf{R}_2)d^3R_2 , \quad (19)$$

where the $\rho^{(m)}$ are the m site distribution functions of the system[48] obeying the normalization condition

$$\frac{1}{V^m}\int\cdots\int \rho^{(m)}(\mathbf{R}_1,\ldots,\mathbf{R}_m)d^3R_1\cdots d^3R_m = 1 \quad (20)$$

and V is the volume of the system. All the integrals in Eq. (19) are well behaved because the singularities in the dipole-dipole interaction tensors are taken care of by the correlation functions which vanish when two spheres approach each other at a distance smaller than their diameter.

Looking at the first integral in the rhs of Eq. (19) one realizes that the most important correlations are the ones between particles 1 and 2 and particles 2 and 3 since the dipolar interaction $\overleftrightarrow{\mathbf{T}}_{ij}$ diverges when $R_{ij}\to 0$. Therefore in order to keep our analysis as simple as possible but at the same time maintaining the main two-particle correlations, we will further assume that

$$\rho^{(3)}(\mathbf{R}_1,\mathbf{R}_2,\mathbf{R}_3)\simeq\rho^{(2)}(\mathbf{R}_1,\mathbf{R}_2)\rho^{(2)}(\mathbf{R}_2,\mathbf{R}_3) . \quad (21)$$

Using this approximation together with Eqs. (18) and (19) we obtain that $\tilde{\alpha}^*$ obeys the extremely simple equation

$$\tfrac{1}{4}f_e\tilde{\alpha}(\tilde{\alpha}^*)^2-\tilde{\alpha}^*+\tilde{\alpha}=0 , \quad (22a)$$

where we introduced the effective filling fraction

$$f_e = 3f\int_0^\infty \frac{\rho^{(2)}(2a_0X)}{X^4}dX . \quad (22b)$$

The solution of Eq. (22) in terms of f_e is

$$\frac{\alpha^*}{2}=\frac{1-(1-f_e\tilde{\alpha}^2)^{1/2}}{f_e\tilde{\alpha}}\underset{f_e\to 0}{\to}\frac{\tilde{\alpha}}{2}\left[1+\frac{f_e}{4}\tilde{\alpha}^2+\cdots\right] , \quad (23)$$

where we have chosen the minus sign before the square root so that $\alpha^*\to\alpha$ when $f_e\to 0$. This means that in the low-density limit we recover the CM relation which served as our starting point. Here we will not question the validity of CM in the low density regime. This problem as well as the possible corrections to Eq. (22) and a systematic comparison with other theories will be reported elsewhere through the development of a diagrammatic approach.[49]

Equations (22) and (23) show that $\tilde{\alpha}^*$ depends not only on $\tilde{\alpha}$ but also on f_e, which has an explicit linear dependence on f and also a nontrivial implicit dependence through a functional of $\rho^{(2)}$. However, it can be easily seen that for a given filling fraction, systems with a tendency towards clustering (when the correlation function has large values for small distances) have a larger f_e than systems with the opposite tendency due to the X^{-4} factor in Eq. (22b).

III. APPLICATIONS

In this section we first analyze the dissipation process contained in Eq. (23). We do this by studying a system of Drude spheres embedded in dispersionless gelatin. We choose for the gelatin $\epsilon_b=2.37$ and for the spheres

$$\epsilon_s(\omega)=1-\omega_p^2/\omega(\omega+i/\tau) , \quad (24)$$

where ω_p is the plasma frequency and τ the relaxation time.

Let us now look at the limit $\tau\to\infty$. In this limit the imaginary part of the sphere polarizability $\tilde{\alpha}=(\epsilon_s-\epsilon_b)/(\epsilon_s+2\epsilon_b)$ is a δ function located at $\omega=\omega_p/\sqrt{1+2\epsilon_b}$. This corresponds to the existence of an electromagnetic mode associated with charge accumulation at the interface between a single sphere and the background. For this reason this mode is called a surface plasmon mode.

In the many-sphere system within the CM approximation ϵ_M is given by Eq. (15) with $\tilde{\alpha}^*=\tilde{\alpha}$. It can be shown that in the $\tau\to\infty$ limit $\mathrm{Im}\epsilon_M$ has a δ-function peak located at

$$\omega_p/\sqrt{1+\epsilon_b(2+f)/(1-f)} .$$

The position of this peak coincides, in the extreme low-density limit ($f\to 0$), with the frequency of the surface-plasmon mode of an isolated sphere and it becomes red shifted with increasing f. The interpretation of this δ-function peak is the existence of a single optically active ($q\to 0$) surface-plasmon mode associated with the system as a whole in which the charge accumulates at the interface between the spheres and the background. The reason for this is that in the CM approximation the dipoles induced in all the spheres are the same and equal to the average dipole, and since in the long-wavelength limit ($q\to 0$) all the dipoles are in phase and the system is isotropic then only one longitudinal mode is possible. Therefore the system within the CM approximation is more similar to an ordered crystal than to a disordered system.

The effect of the relaxation time (finite τ) in the Drude dielectric function is the broadening of the δ-function surface-plasmon peak and it can be easily shown that this broadening is independent of f within the CM approximation. On the other hand, in Eq. (23), even in the $\tau\to\infty$ limit, $\tilde{\alpha}^*$ will acquire an imaginary part in the continuous frequency region in which $\tilde{\alpha}^2(\omega)\geq 1/f_e$. Since ϵ_b is real, Eq. (15) tells us that ϵ_M has an imaginary part whenever $\tilde{\alpha}^*$ does. This indicates the presence in the system of optically active ($q\to 0$) surface-plasmon modes with frequencies distributed in a continuous range. The presence of those modes is directly related to the fact that one is dealing with a disordered system which allows dipolar fluctuations in a continuous fashion. It also shows that our approximation for α^* takes into account the occurrence of those fluctuations. As a consequence one will obtain a broad surface-plasmon peak in $\mathrm{Im}\epsilon_M(\omega)$

within the frequency region defined by $\tilde{\alpha}^2(\omega) \geq 1/f_e$.

In order to examine the dependence of our results on the two-site distribution function, we calculate f_e for three different choices of $\rho^{(2)}(X)$: the hole correction (HC), Percus Yevick (PY), and molten copper (MCu). For the case of the HC, $\rho^{(2)}(X)=\theta(X-1)$, where θ is the unit step function; for PY we used the definition given in Ref. 50; and for MCu we used the distribution function corresponding to $f=0.25$ as described in Ref. 1, where a Monte Carlo technique was used to smooth out the experimental data.[51] PY is similar to HC for small f (≤ 0.1), but it differs more and more from HC when f increases, as is shown in Fig. 2 of Ref. 10.

In Fig. 1 we show f_e as a function of f. As it can be seen, for HC we get $f_e=f$ and for PY we get that f_e is larger than f for all f. The dot shows the value of f_e for MCu at $f=0.25$. In Fig. 2 we show a plot of $\tilde{\alpha}^2$ as a function of ω for the system described above in the $\tau \to \infty$ limit. The two arrows indicate the frequencies of the CM δ-function absorption peaks for $f=0.1$ and 0.3. The latter one is red shifted with respect to the first one. The horizontal solid (dashed) lines are located at $1/f_e$ for the HC (PY) distribution function for $f=0.1$ and 0.3. Their length indicates the frequency window in which $\tilde{\alpha}^2 \geq 1/f_e$. One can see that the bigger f_e the wider the frequency region of optically active modes. This region lies asymmetrically about the CM δ-function located at $\tilde{\alpha}^2=1/f^2$. Thus when f and f_e decrease the frequency region shrinks around the CM peak which, at the same time, moves towards the location of the single-sphere resonance. The effect of a finite relaxation time in the Drude dielectric function [Eq. (24)] will be to provide an additional broadening of the surface-plasmon peak due to the damping of the modes. The line shape of this peak can be obtained immediately by combining Eqs. (15), (22b), and (23). It can be seen that it depends separately on f and f_e.

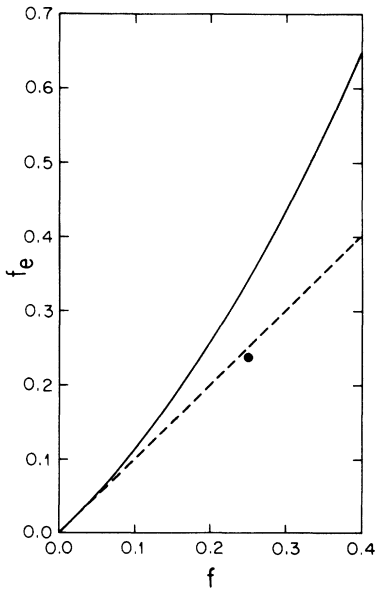

FIG. 1. Values of f_e as a function of f. The dashed (solid) line is obtained when one uses the HC (PY) pair distribution function in Eq. (22b). The dot at $f=0.25$ is the value of f_e when one uses the MCu distribution function.

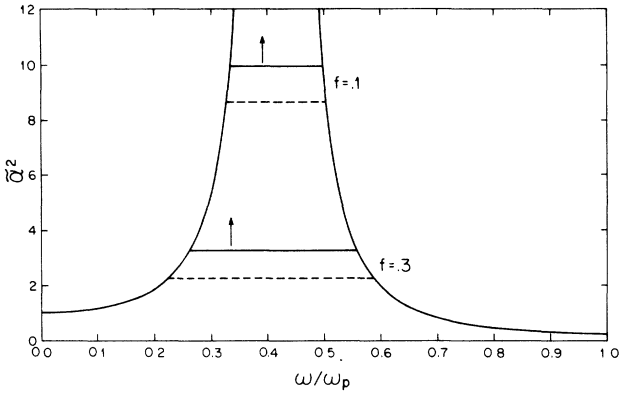

FIG. 2. Curves are $\tilde{\alpha}^2$ as a function of ω/ω_p for Drude spheres in gelatin ($\epsilon_b=2.37$) and $\tau \to \infty$. The horizontal solid (dashed) lines are located at $1/f_e$ for HC (PY) and their length represents the interval of frequencies for which α^* has an imaginary part. The upper (lower) pair of horizontal lines corresponds to $f=0.1$ ($f=0.3$). The arrows indicate the position of the CM δ-function absorption peaks.

In Fig. 3 we plot $\mathrm{Im}\epsilon_M$ as a function of ω for the same model of Drude spheres described above. We choose a finite relaxation time $\tau=92/\omega_p$ and two volume fractions $f=0.1$ and 0.3. The solid (dashed) lines correspond to the HC (PY) distribution function. The curves for $f=0.3$ are red shifted with respect to the ones for $f=0.1$. As a reference we also show with arrows the position of the CM peaks for $f=0.1$ and 0.3. It can be seen that the peaks are considerably broader than the CM ones and highly asymmetric, showing a greater weight for

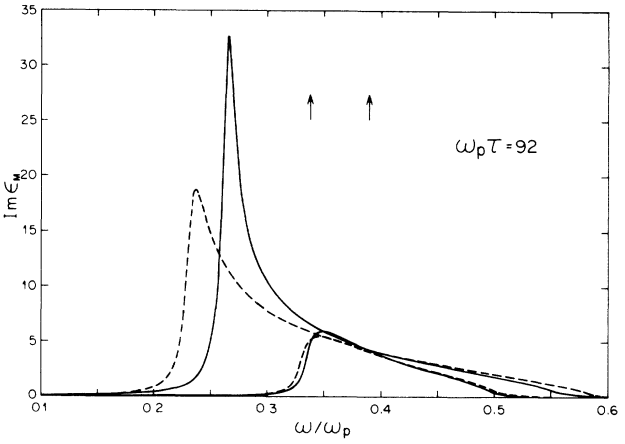

FIG. 3. Imaginary part of ϵ_M as a function of ω for Drude spheres in gelatin ($\epsilon_b=2.37$) and two different volume fractions ($f=0.1$ and 0.3). Here $\omega_p\tau=92$. The solid (dashed) lines correspond to HC (PY) correlation function and the arrows indicate the position of the peaks of MGT. The curves for $f=0.3$ are red shifted with respect to the ones for $f=0.1$.

the low-frequency modes. Furthermore, they span over a frequency region which goes slightly beyond the one displayed in Fig. 2 due to the finite relaxation time. The curves corresponding to the PY distribution function undergo a larger red shift than the ones with HC. The difference between them is more prominent as f increases. This means that for large f our results are more sensitive to the choice of the distribution function, thus a detailed comparison with experiment has to take this fact into account. It also shows that for the same f the effects of clustering (larger f_e) imply a larger red shift of the $\mathrm{Im}\epsilon_M$ peak.

In order to examine the dependence of the line shape of the surface-plasmon peak on the relaxation time, in Fig. 4 we plot $\mathrm{Im}\epsilon_M$ as a function of ω for the same parameters as in Fig. 3 but now choosing $\tau=46/\omega_p$. The main effect is a reduction in the size of the peaks and a larger broadening at half-maximum. Since for a small enough sphere τ is a function of its radius due to surface scattering, the only dependence on the size of the spheres which appears in this theory is through τ. As in Fig. 3, the position of the CM peaks for $f=0.1$ and 0.3 are shown with arrows.

The choice of parameters in Fig. 4 also correspond to the same parameters chosen in Ref. 9, where a theory based on the lattice-gas coherent-potential approximation (LG-CPA) was developed. Thus we can make a direct comparison between our theory and LG-CPA. In the latter the spatial disorder is not described by distribution functions but is replaced by substitutional disorder in a cubic lattice. In Fig. 4 the open (solid) circles correspond to the results of LG-CPA for $f=0.1$ ($f=0.3$) in a fcc lattice. It can be seen that for $f=0.1$ the line shape of the peaks in both theories are quite similar although LG-CPA shows a slightly larger red shift. For $f=0.3$ the results of LG-CPA lie very close to ours for the case of the HC distribution function, but they differ markedly from the ones calculated with PY which are now red shifted with respect to both.

In Fig. 5 we summarize our results for the lineshape of $\mathrm{Im}\epsilon_M$ by plotting the frequency of the surface-plasmon peak $\omega_{\mathrm{peak}}/\omega_p$ as a function of the volume fraction of

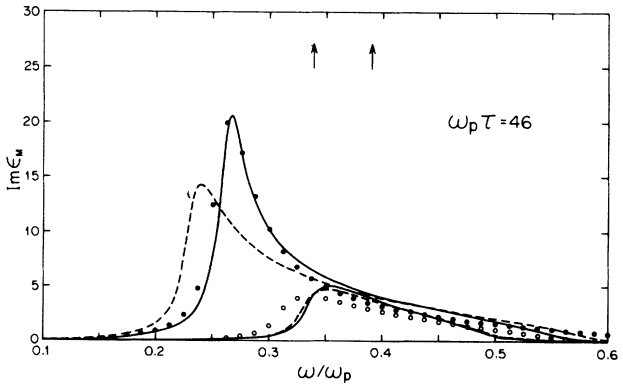

FIG. 4. Same as Fig. 3 but with $\omega_p\tau=46$. The open (closed) circles correspond to LG-CPA for $f=0.1$ ($f=0.3$).

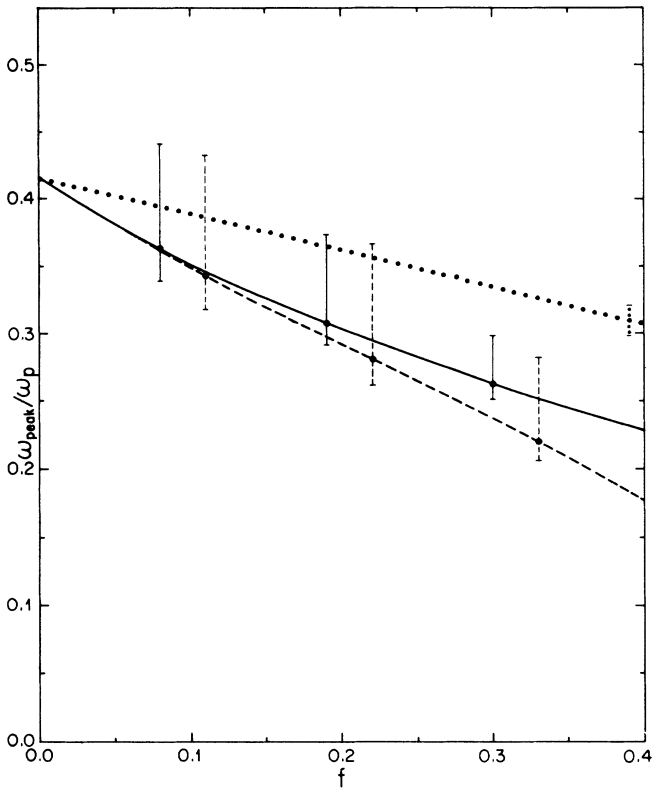

FIG. 5. Dotted line is the position of the peak as a function of f predicted by the MGT. The solid (dashed) line is the corresponding position of the peak according to our theory using the correlation function HC (PY). The vertical lines represent the full width of the peak at half maximum at some values of f. The width of MGT is the same for all values of f.

spheres for the HC and PY distribution functions. The position of the peak in MGT is also shown. The vertical bars are the full width of the peak at half maximum (FWHM). We can see that the position of the peaks for both HC and PY are red shifted with respect to MGT for all f. Also, for the same f the peak for PY is red shifted with respect to the one for HC. Since f_e is greater for PY than for HC (for all f), one can say that clustering (larger f_e) amounts to a larger red shift.

Now we compare the results of our theory with the effective-medium approximation (EMA) of Davis and Schwartz.[1,4] In their theory the spatial disorder is described through distribution functions and they take into account the contribution of induced dipoles and also higher multipoles. They reported[4] results for a system of silver spheres embedded in gelatin ($\epsilon_b=2.37$) using

$$\epsilon_s(\omega)=\epsilon_0-\omega_p^2/(\omega^2+i\omega/\tau)\ ,$$
$$\epsilon_0=5.95,\quad \hbar\omega_p=9.2\ \mathrm{eV},\quad \hbar/\tau=0.1\ \mathrm{eV}\ . \tag{25}$$

In Fig. 6 we show their results for $\mathrm{Im}\epsilon_M(\omega)$ and $f=0.21$. The open (solid) dots correspond to the dipolar contribution for the PY (MCu) distribution function.[51] In their calculation the MCu function corresponding to $f\simeq 0.25$ was rescaled in order to treat the case $f=0.21$ where recent experimental data are available. The solid

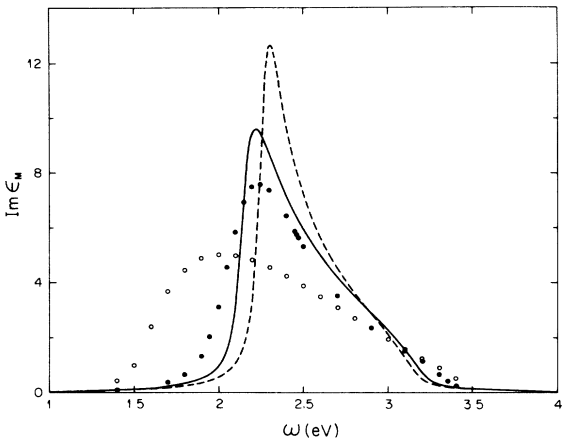

FIG. 6. Same as Fig. 3 but with $f=0.21$ and for silver spheres with $\epsilon_s(\omega)=5.95-\omega_p^2/(\omega^2+i\omega/\tau)$. Here $\hbar/\tau=0.1$ eV. The solid (dashed) line is our result corresponding to the PY (MCu) correlation function. The circles are the dipolar contribution of EMA for the same system. The open (closed) circles correspond to the PY (MCu) correlation function.

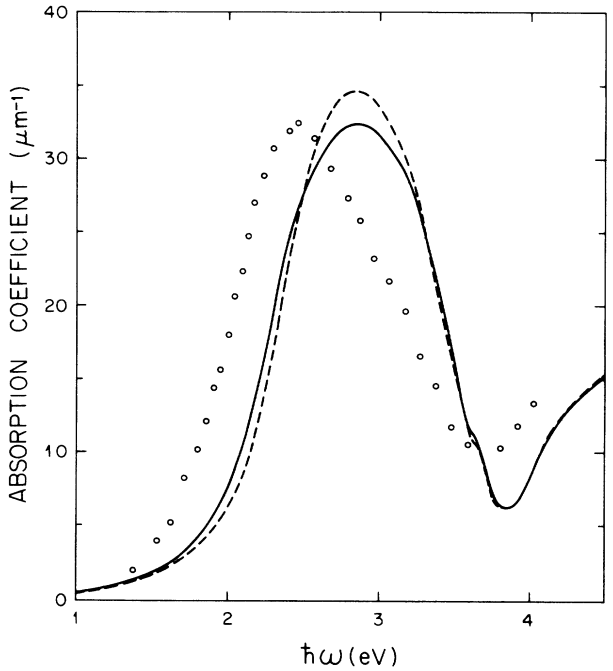

FIG. 7. Absorption coefficient $(2\omega/c)\mathrm{Im}\sqrt{\epsilon_M}$ of Ag particles embedded in gelatin with $f=0.21$. The solid (dashed) line correspond to the PY (HC) correlation function. The dots are the experimental results arbitrarily normalized.

(dashed) line is our result for $f=0.21$ using the same dielectric functions (Eq. (25) and the same PY (MCu) distribution function as Davis and Schwartz.[4,51] In order to have a direct comparison of both theories we also used their same scaling procedure for MCu, although this procedure might be questionable. As it can be seen, the way in which the results of the two theories depends on the choice of the distribution function is appreciably different. However, our results with PY are similar to the ones of EMA but with MCu. Also, our results with MCu (dashed line) do not differ appreciably from our results with HC (not show in the figure), because for MCu the value of f_e (0.1996) is very close to the one for HC ($f_e=f$). Since in our theory the dependence on the distribution function is through the integral of Eq. (22b), which samples $\rho^{(2)}$ only around $2a_0$, two different distribution functions might have similar values of f_e.

Finally, in Fig. 7 we show a comparison of our theoretical results with the experimental absorption coefficient $\beta=2\omega\,\mathrm{Im}\sqrt{\epsilon_M}/c$ of a system of silver spheres in gelatin at a volume fraction of 0.21.[25] For this calculation we chose $\epsilon_b=2.37$ and the dielectric function of the spheres was taken directly from the experimental values of bulk silver,[52] but with an adjusted relaxation time of $\hbar/\tau=0.6$ eV in the Drude contribution to take into account the size and the defects in the silver particles.[53] We show results for HC and PY distribution functions and the experimental results are arbitrarily normalized. We can see that the comparison with experiment is very sensitive to the choice of the distribution function and our results show a slightly better agreement for PY.

IV. CONCLUSIONS

We have developed a simple theory for the macroscopic dielectric function ϵ_M of a system of identical spheres with a local dielectric function ϵ_s embedded in a medium with a local dielectric function ϵ_b within the dipolar, nonretarded limit. The main approximation of the theory is the assumption that the polarization of each sphere is proportional to the sum of the external field and the fluctuating field produced by average dipoles located at random positions. The proportionality constant α^* was obtained self-consistently in order to account for the dipolar fluctuations. The relationship between ϵ_M, ϵ_s, and ϵ_b is similar to MGT but with the renormalized polarizability α^* instead of the bare polarizability α of the spheres. The renormalized polarizability α^* obeys a second-order algebraic equation and is given in terms of α and a parameter f_e which is a functional of the two-particle distribution function of the spheres.

We applied our theory to a system of Drude spheres embedded in dispersionless gelatin, and we analyzed the position and the line shape of the surface-plasmon peak in $\mathrm{Im}\epsilon_M$. We conclude that for volume fractions greater than or equal to 0.2 the position and the shape of the peak is very sensitive to the choice of the two-particle distribution function. We also obtained that clustering (larger f_e) will produce a larger red shift of the peak.

A comparison of our results for $\mathrm{Im}\epsilon_M(\omega)$ with other theories shows that for $f\sim 0.3$ they agree rather well with the ones of LG-CPA (Ref. 9) when we choose HC as the correlation function. However, the use of PY yields a larger red shift than LG-CPA. For smaller f our results are not as sensitive to the choice of distribution function and LG-CPA shows a larger red shift of the surface-plasmon peak than our results. When we compare our calculations with the ones of effective-mass approximation[1,4] (EMA), we find that for $f=0.21$ the dependence

of $\mathrm{Im}\epsilon_M(\omega)$ on the choice of the distribution function has distinctive differences. Nevertheless, both theories can achieve a reasonable agreement with experimental results[25] with an appropriate choice of the distribution function. Therefore a more meaningful comparison with experiment will require an experimentally determined two-site distribution function. A better description of the dielectric function of the particles, the inclusion of higher multipoles, and an appropriate average over the distribution of sizes and shapes of the particles found on the experimental system are also necessary. The effects of quadrupole interactions have been already calculated within the EMA.[1,2] A slightly larger red shift of the plasmon peak is obtained when the quadrupole interactions are included, especially at high volume fraction (0.3–0.4). Some of the consequences of nonuniform size distribution as well as an extension to two-dimensional systems have been reported within LG-CPA.[9,54] The nonuniformity of particle sizes seems[9] to enhance the broadening of the plasmon peak, while its redshift relative to the MGT position is slightly reduced.

Due to the simplicity of our theory it will be rather straightforward to include retardation, higher multipoles, and to explore the consequences of size distribution as well as its extension to $2D$ adsorbed monolayers. The comparison of our theory with others as well as with a wider variety of experimental results will be also desirable. The calculations that we have performed so far are already promising and we believe they can stimulate further research in the field.

ACKNOWLEDGMENTS

We would like to acknowledge fruitful conversations with Enrique Anda, Ronald Fuchs, Esteban Martina, and José Luis Morán-López. We are also grateful to Pedro Villaseñor and Victoria Davis for sending us the raw data and all the additional information that we required for comparing our results with theirs. This work was supported in part by Consejo Nacional de Ciencia y Tecnología (México) through Grant No. PCEXCNA-040428.

*Permanent address: Instituto de Física, Universidad Autónoma de México, Apartado Postal 20-364, 01000 México, Distrito Federal, México.

[1]V. A. Davis and L. Schwartz, Phys. Rev. B **33**, 6627 (1986).
[2]A. Wachniewski and H. B. McClung, Phys. Rev. B **33**, 8053 (1986).
[3]B. U. Felderhof and R. B. Jones, Z. Phys. B **62**, 231 (1986); **62**, 225 (1986); **62**, 215 (1986).
[4]V. A. Davis and L. Schwartz, Phys. Rev. B **31**, 5155 (1985).
[5]M. Gómez, L. Fonseca, G. Rodríguez, A. Velázquez, and L. Cruz, Phys. Rev. B **32**, 3429 (1985).
[6]B. U. Felderhof and R. B. Jones, Z. Phys. B **62**, 43 (1985).
[7]G. S. Agarwal and R. Ingura, Phys. Rev. B **30**, 6108 (1984).
[8]A. Bittar, S. Berthier, and J. Lafait, J. Phys. (Paris) **45**, 623 (1984).
[9]A. Liebsch and P. Villaseñor, Phys. Rev. B **29**, 6907 (1984); B. N. J. Persson and A. Liebsch, Solid State Commun. **44**, 1637 (1982); J. Phys. C **16**, 5375 (1983).
[10]L. Tsang and J. A. Kong, J. Appl. Phys. **53**, 7162 (1982).
[11]B. U. Felderhof, G. W. Ford, and E. G. D. Cohen, J. Stat. Phys. **28**, 649 (1982); **28**, 135 (1982).
[12]D. J. Bergman and S. Stroud, Phys. Rev. B **22**, 3527 (1980).
[13]G. W. Milton, Appl. Phys. Lett. **37**, 300 (1980).
[14]L. Tsang and J. A. Kong, J. Appl. Phys. **51**, 3465 (1980).
[15]P. Sheng, Phys. Rev. Lett. **45**, 60 (1980).
[16]D. J. Bergman, Phys. Rev. Lett. **44**, 1285 (1980).
[17]W. Lamb, D. M. Wood, and N. W. Aschcroft, Phys. Rev. B **21**, 2248 (1980).
[18]D. Stroud and F. P. Pan, Phys. Rev. B **17**, 1602 (1978).
[19]D. J. Bergman, Phys. Rep. **43**, 377 (1978).
[20]M. Quinten and U. Kreibig, Surf. Sci. **172**, 557 (1986).
[21]W. J. Kaiser, E. M. Lagothetis, and L. E. Wenger, Solid State Commun. **58**, 83 (1986).
[22]K. D. Cummings, J. C. Garland, and D. B. Tanner, Phys. Rev. **30**, 4170 (1984).
[23]S. Berthier and J. Lafait, Thin Solid Films **89**, 213 (1982).
[24]W. G. Egan and D. E. Aspnes, Phys. Rev. B **26**, 5313 (1982).
[25]U. Kreibig, A. Althoff, and H. Pressmann, Surf. Sci. **106**, 308 (1981); U. Kreibig, Z. Phys. B **31**, 39 (1978).
[26]C. G. Granqvist and O. Hunderi, Phys. Rev. B **16**, 3513 (1977).
[27]J. I. Gittleman and B. Abeles, Phys. Rev. B **15**, 3273 (1977).
[28]E. B. Priestley, B. Abeles, and R. W. Cohen, Phys. Rev. B **12**, 2121 (1975).
[29]R. W. Cohen, G. D. Cody, M. D. Coutts, and B. Abeles, Phys. Rev. B **8**, 3689 (1973).
[30]J. C. Maxwell Garnett, Philos, Trans. R. Soc. Lond **203**, 385 (1904).
[31]See, for example, C. G. Granqvist, J. Appl. Phys. **50**, 2916 (1979).
[32]J. E. Gubernatis, in *Electrical Transport and Optical Properties of Inhomogeneous Media (Ohio State University, 1977)*, Proceedings of the First Conference on the Electrical Transport and Optical Properties of Inhomogeneous Media, AIP Conf. Proc. No. 40, edited by J. C. Garland and D. B. Tanner (AIP, New York, 1978), p. 84.
[33]J. Korringa, J. Phys. Chem. Solids **7**, 252 (1958).
[34]M. Lax, Phys. Rev. **85**, 621 (1952).
[35]N. C. Mathur and K. C. Yeh, J. Math. Phys. **5**, 1619 (1964); P. C. Waterman and R. Truell, *ibid.* **2**, 512 (1961).
[36]D. E. Aspnes, Am. J. Phys. **50**, 704 (1982).
[37]R. Clausius, *Die mechanische Behandlung der Electrizität* (Vieweg, Braunschweig, 1879), p. 62; H. A. Lorentz, *The Theory of Electrons* (Dover, New York, 1952); *Dictionary of Scientific Biography*, edited by C. C. Guillespie (Scribner's, New York, 1974), Vol. IX, p. 547.
[38]J. G. Kirkwood, J. Chem. Phys. **4**, 592 (1936); J. de Boer, F. Van der Maesen, and C. A. Ten Seldam, Physica (Utrecht) **19**, 265 (1953); A. Isihara, J. Chem. Phys. **38**, 3437 (1963); D. A. McQuarrie and H. B. Levine, Physica (Utrecht) **31**, 749 (1965); J. D. Ramshaw, *ibid.* **62**, 1 (1972); B. R. A. Nijboer, Physica A **80**, 398 (1975).
[39]A. Isihara and R. V. Hanks, J. Chem. Phys. **36**, 433 (1962).
[40]M. S. Wertheim, Mol. Phys. **25**, 211 (1973); M. S. Wertheim, Ann. Rev. Phys. Chem. **30**, 471 (1979).
[41]L. Rosenfeld, *Theory of Electrons* (North-Holland, Amster-

dam, 1951), Chap. VI; P. Mazur, *Advances in Chemical Physics* (Interscience, New York, 1958), Vol. 1, p. 309; R. K. Bullough, J. Phys. A (Proc. Phys. Soc.) Ser. 2 **1**, 409 (1968); F. Hynne and R. K. Bullough, J. Phys. A **5**, 1272 (1972); D. Bedeaux and P. Mazur, Physica (Utrecht) **67**, 23 (1973).

[42]P. Mazur and M. Mandel, Physica (Utrecht) **22**, 299 (1956).

[43]See, for example, F. García-Moliner and F. Flores, *Introduction to the Theory of Solid Surfaces* (Cambridge University Press, London, 1979), Chap. 1.

[44]W. L. Mochán and R. G. Barrera, Phys. Rev. B **32**, 4989 (1985).

[45]J. D. Ramshaw, Physica (Utrecht) **62**, 1 (1972).

[46]See, for example, R. G. Barrera and P. A. Mello, Am. J. Phys. **50**, 165 (1982).

[47]See, for example, J. D. Jackson, *Classical Electrodynamics,* 2nd ed. (Wiley, New York, 1975), p. 155.

[48]D. A. McQuarrie, *Statistical Mechanics* (Harper and Row, New York, 1976), Chap. 13.

[49]R. G. Barrera, G. Monsivais, W. L. Mochán, and E. Anda (unpublished).

[50]M. S. Wertheim, Phys. Rev. Lett. **10**, 321 (1963).

[51]V. Davis (private communication).

[52]P. B. Johnson and R. W. Christy Phys. Rev. B **6**, 4370 (1972).

[53]Quoted from U. Kreibig in Ref. 9. For the Drude contribution in bulk silver we took $\hbar/\tau=0.025$ eV.

[54]B. N. J. Persson and A. Liebsch, Phys. Rev. B **28**, 4247 (1983).